# Structure/Reactivity Relationships in the Unimolecular Gas-Phase Chemistry of Dialkyl Peroxide/$Fe^+$ Complexes

**Christoph A. Schalley, Ralf Wesendrup, Detlef Schröder, Katrin Schroeter, and Helmut Schwarz***

*Contribution from the Institut für Organische Chemie der Technischen Universität Berlin, D-10623 Berlin, Germany*

*Received June 6, 1995*[⊗]

**Abstract:** Unimolecular and collision-induced fragmentations of dialkyl peroxide/$Fe^+$ complexes, ROOR′/$Fe^+$ (R, R′ = methyl, ethyl, isopropyl, *tert*-butyl), were examined by means of tandem mass spectrometry. In the initial reaction step, iron bis(alkoxide) ions (RO)Fe(OR′)$^+$ are generated by insertion of the metal cation into the weak O−O bond of the peroxide. Depending on the nature of R and R′, five major reaction channels have been observed, corresponding to the generation of a methyl radical, methane, and water. Kinetic isotope effects are determined and interpreted in terms of rate-determining steps of the multistep processes. The observed reactivity can be described as a result of the balance of the energetics of $\beta$-hydrogen *versus* $\beta$-methyl shifts together with product stabilities. A scheme is presented, which correlates the unimolecular reactivity of ROOR′/$Fe^+$ complexes with the substitution pattern in the $\alpha$- and $\beta$-positions of the peroxidic alkyl groups.

## Introduction

Catalytic oxidation of organic substrates, in particular the functionalization of saturated hydrocarbons, constitutes one of the most interesting fields in transition-metal chemistry.[1] These processes not only are of enormous economic interest, but also represent the key steps in some biochemical transformations,[2] as for example in the oxidation of methane by methane monooxygenase[3] or the P-450-mediated hydroxylation reactions.[4] Nevertheless, often the mechanistic aspects are not very well understood and the elementary steps are even unknown in many cases, since ligand and complicating bulk effects render a detailed analysis of the microscopic events difficult. In this respect, gas-phase studies provide insight into the mechanisms of these processes as well as probe the intrinsic properties of transition-metal cations.[5] Ultimately, it is hoped that these efforts will contribute to the understanding of reactivity patterns in applied transition-metal catalysis and eventually may help to develop tailor-made catalysts.

Despite the importance of peroxo compounds in both technical processes[6] and small-scale organic synthesis[7] and the role they play as key intermediates in biosyntheses,[8] the gas-phase chemistry of metal cations with organic peroxides has been almost completely neglected so far.[9,10] Therefore, a systematic mass spectrometric investigation of peroxide/$M^+$ complexes is indicated, and to this end, recently we have screened the bimolecular reactions of dimethyl peroxide with bare $M^+$ cations, including nearly all first-, second-, and third-row transition metals.[11] In addition, a more detailed comparison of the bi- and unimolecular chemistry of dimethyl peroxide with $Cr^+$, $Mn^+$, $Fe^+$, and $Co^+$ has been conducted.[12]

In this article, we will address the influence of the alkyl groups in dialkyl peroxides ROOR′ (R, R′ = methyl, ethyl, isopropyl, *tert*-butyl) on the unimolecular reactivities of their corresponding peroxide/$Fe^+$ complexes. As will be shown, the substitution pattern at the $\alpha$-position is crucial for the fragmentation behavior of ROOR′/$Fe^+$. The investigation of the compounds shown in Charts 1 and 2 not only provides mechanistic information; in addition, a simple predictive concept emerges which describes the reactivity of dialkyl peroxide/$Fe^+$ complexes in terms of the peroxide structure. In the following, we will use R for the less substituted alkyl group as compared to R′ (i.e., R ≤ R′).

## Experimental Section

The experiments were performed with a modified VG ZAB/HF/AMD four-sector mass spectrometer of BEBE configuration (B stands for magnetic and E for electric sectors), which has been described previously.[13] Briefly, a mixture of the peroxide and $Fe(CO)_5$ was ionized by a beam of electrons having 50−100 eV kinetic energy in a chemical ionization (CI) source. To avoid peroxide decomposition, a

[⊗] Abstract published in *Advance ACS Abstracts,* December 1, 1995.

(1) (a) Shilov, A. E. *Activation of Saturated Hydrocarbons by Transition Metal Complexes*, Reidel: Dordrecht, The Netherlands, 1984. (b) Hill, C. G. *Activation and Functionalization of Alkanes*; Wiley: New York, 1989. (c) Also see: Barton, D. H. R., Martell, A. E., Sawyer, D. T., Eds. *The Activation of Dioxygen and Homogeneous Catalytic Oxidation*; Plenum Press: New York, 1993.

(2) Lippard, S. J.; Berg, J. M. *Principles of Bioinorganic Chemistry*; University Science Books: Mill Valley, CA 1994.

(3) (a) Liu, K. E.; Johnson, C. C.; Newcomb, M.; Lippard, S. J. *J. Am. Chem. Soc.* **1993**, *115*, 939. (b) Lee, S.-K.; Nesheim, J. C.; Lipscomb, J. D. *J. Biol. Chem.* **1993**, *268*, 21569.

(4) Ortiz de Montellano, P. R., Ed. *Cytochrome P-450: Structure, Mechanism, and Biochemistry*; Plenum Press: New York, 1986.

(5) (a) Armentrout, P. B. *Annu. Rev. Phys. Chem.* **1990**, *41*, 313. (b) Eller, K.; Schwarz, H. *Chem. Rev.* **1991**, *91*, 1121. (c) Eller, K. *Coord. Chem. Rev.* **1993**, *126*, 93. (d) Freiser, B. S. *Acc. Chem. Res.* **1994**, *27*, 353.

(6) (a) Hock, H.; Kropf, H. *Angew. Chem.* **1957**, *69*, 313. (b) For a recent example of methane coupling in the presence of hydrogen peroxide, see: Iskendirov, I.; Sokolovskii, V.; Coville, N. *J. Chem. Soc., Chem. Commun.* **1994**, 2033.

(7) (a) Sharpless, K. B. *Chem. Brit.* **1986**, 38. (b) Pfenninger, A. *Synthesis* **1986**, 89. (c) Adam, W.; Richter, M. J. *Acc. Chem. Res.* **1994**, *27*, 57.

(8) Adam, W.; Bloodworth, A. J. *Ann. Rep. B, Chem. Soc.* **1978**, 342.

(9) Hisatome, M.; Yamakawa, K. *Org. Mass Spectrom.* **1978**, *13*, 1.

(10) For a review of the mass spectrometry of metal-free peroxides, see: Schwarz, H.; Schiebel, H.-M. In *The chemistry of peroxides*; Patai, S., Ed., Wiley: New York, 1983; p 105.

(11) Wesendrup, R.; Schalley, C. A.; Schröder, D.; Schwarz, H. *Chem. Eur. J.*, in press.

(12) Schalley, C. A.; Wesendrup, R.; Schröder, D.; Weiske, T.; Schwarz, H. *J. Am. Chem. Soc.* **1995**, *117*, 7711.

(13) (a) Srinivas, R.; Sülzle, D.; Weiske, T.; Schwarz, H. *Int. J. Mass Spectrom. Ion Processes* **1991**, *107*, 368. (b) Srinivas, R.; Sülzle, D.; Koch, W.; DePuy, C. H.; Schwarz, H. *J. Am. Chem. Soc.* **1991**, *113*, 5970.

0002-7863/95/1517-12235$09.00/0 

## Chart 1

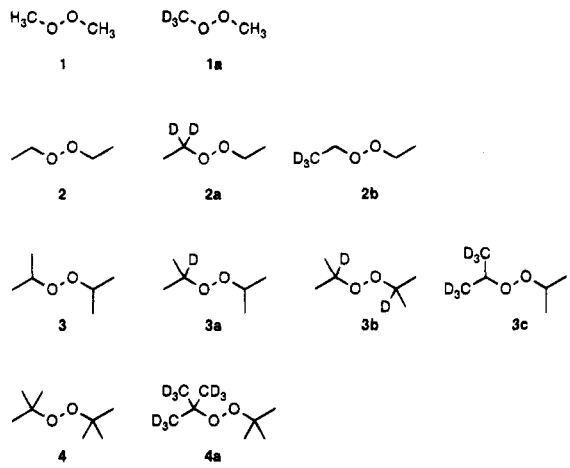


## Chart 2

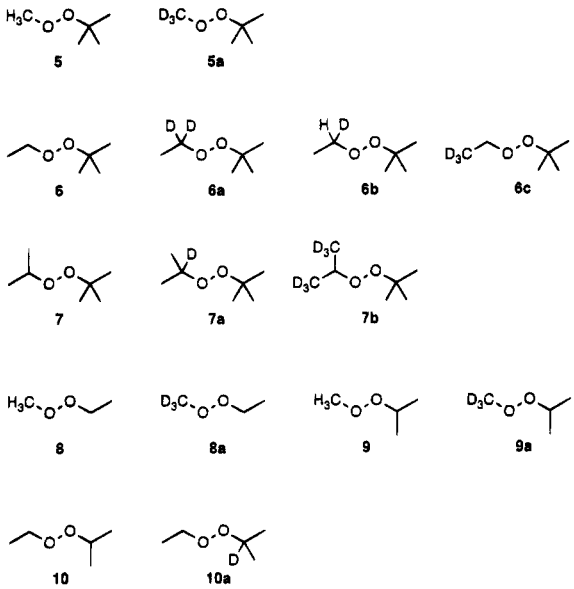


metal-free Teflon/glass inlet system was used for the introduction of the peroxides into the ion source, while $Fe(CO)_5$ was leaked-in *via* a heated septum inlet system (70 °C). The ions were accelerated to 8 keV translational energy and mass-selected by means of B(1)/E(1) at a resolution of $m/\Delta m$ 3000−6000, which was sufficient to separate the ions of interest from isobaric impurities. Unimolecular fragmentations of metastable ions (MI) occurring in the field-free region preceding B(2) were recorded by scanning this sector. For collisional activation (CA) experiments mass-selected ions were collided with helium (80% transmission, T). The error of the relative intensities in MS/MS experiments does not exceed ±5%. MS/MS/MS experiments[14] were performed by selecting the fragment ions of interest by means of B(2), and the collision-induced fragmentations (He, 80% T) occurring in the subsequent field-free region were monitored by scanning E(2); these experiments will be referred to as MI/CA spectra. The sensitivity in MS/MS/MS experiments is less, as compared to that of the MS/MS studies, and the error is estimated to ±15%. The structures of the major ionic products have been characterized by MI/CA spectra, and the discussion of the systems **4**/$Fe^+$ and **4a**/$Fe^+$ may suffice to serve as a representative example for describing these experiments. As a further structural probe, bis-ligated intermediates have been generated independently from authentic precursors. For the sake of brevity, these data are presented only for the $(C_2H_5OH)Fe(CH_3CHO)^+$ complex and some of its deuterated analogues. All spectra were accumulated and

(14) (a) Busch, K. L.; Glish, G. L.; McLuckey, S. A. *Mass Spectrometry/Mass Spectrometry: Techniques and Applications of Tandem Mass Spectrometry*; VCH Publishers: Weinheim, Germany, 1988. (b) Schröder, D.; Schwarz, H. *Int. J. Mass Spectrom. Ion Processes* **1995**, *146/147*, 183.

## Scheme 1

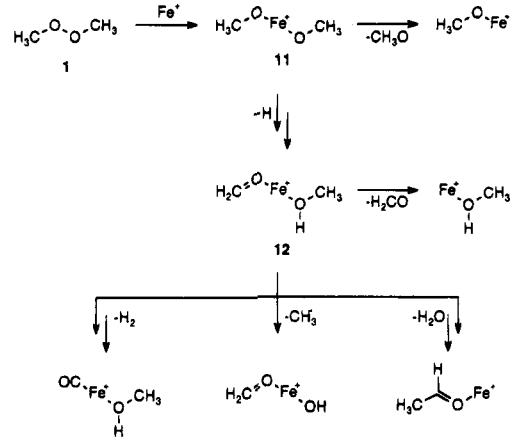


on-line processed with the AMD-Intectra data system; 5−30 scans were averaged to improve the signal-to-noise-ratio.

Di-*tert*-butyl peroxide **4** was used as purchased, and commercially available *tert*-butyl hydroperoxide served as a precursor for the synthesis of the *tert*-butyl-substituted peroxides **5**−**7**. The remaining peroxo compounds were prepared by established laboratory procedures employing deuterium-labeled reagents which contained in general >98 atom % D. Typically, peroxides were synthesized by coupling the corresponding hydroperoxides with (labeled) alkyl bromides using silver trifluoroacetate as the coupling reagent.[15] Isopropyl hydroperoxide, which served as a precursor for these syntheses, was generated similarly from $H_2O_2$, while ethyl hydroperoxide was prepared in higher yields by reacting molecular oxygen with ethyl chloride Grignard reagent and subsequent hydrolysis.[16] **1**, **1a**, **8**, **8a**, **9**, and **9a** were synthesized by alkylation of $H_2O_2$ or the corresponding hydroperoxides with dimethyl sulfate or dimethyl-$d_6$ sulfate under basic conditions.[17] All products were purified by distillation and characterized by their $^1$H-NMR[18] and mass spectra (CI, methane).[10,19]

## Results and Discussion

The gas-phase chemistry of the dimethyl peroxide/$Fe^+$ complexes **1**/$Fe^+$ and **1a**/$Fe^+$ has been discussed in detail elsewhere,[11,12] and Scheme 1 gives an overview of the metastable ion decompositions of **1**/$Fe^+$. For the further discussion, three aspects should be recalled: (i) After insertion of the $Fe^+$ cation into the weak O−O bond (BDE = 37 kcal/mol),[20] the iron(III) bis(methoxide) cation **11** is formed, which can rearrange to the iron(I) complex **12** *via* consecutive hydrogen transfer. The two major neutral products, i.e. $CH_3^\bullet$ (59%) and $H_2O$ (35%), are formed from intermediate **12**. Based on the observed kinetic isotope effects it was concluded that the hydrogen atom transfer **11** → **12** is rate determining for the unimolecular fragmentations of **1**/$Fe^+$. Since in related metal methoxide systems the $\beta$-hydrogen transfer from a methoxy group to the metal center has been reported to be reversible,[21] in the present system, the second step of the two-step migration, i.e. the hydrogen transfer from the metal to the oxygen atom of the other methoxy group, is supposed to be rate determining. (ii) Cleavage of the C−O

(15) Cookson, P. G.; Davies, A. G.; Roberts, B. P. *J. Chem. Soc., Chem. Commun.* **1976**, 1022.
(16) Walling, C.; Buckler, S. A. *J. Am. Chem. Soc.* **1953**, *75*, 4372.
(17) Rieche, A.; Brumshagen, W. *Chem. Ber.* **1928**, *61*, 63.
(18) (a) Sosnovsky, G. S.; Zaret, E. H. *J. Org. Chem.* **1969**, *34*, 968. (b) Kropf, H.; Bernert, C.-R. *Z. Anal. Chem.* **1969**, *248*, 35. (c) Bloodworth, A. J.; Bylina, G. S. *J. Chem. Soc., Perkin Trans 1* **1972**, 2433. (d) Budinger, P. A.; Mooney, J. R.; Grasselli, J. G.; Fay, P. S.; Guttman, A. T. *Anal. Chem.* **1981**, *53*, 884.
(19) Fraser, R. T. M.; Paul, N. C.; Phillips, L. *J. Chem. Soc. (B)* **1970**, 1278.
(20) (a) Shaw, D. H.; Pritchard, H. O. *Can. J. Chem.* **1968**, *46*, 2722. (b) Batt, L.; McCullough, R. D. *Int. J. Chem. Kinet.* **1976**, *8*, 911.
(21) Cassady, C. J.; Freiser, B. S. *J. Am. Chem. Soc.* **1985**, *107*, 1566.

**Table 1.** Mass Differences ($\Delta m$ in amu) Observed in the MI Mass Spectra of $Fe^+$ Complexes of Symmetric Dialkyl Peroxides **1**–**4** and Their Isotopologues[a]

| | $\Delta m$ | | | | | | | | | | | | | | | | |
|---|---|---|---|---|---|---|---|---|---|---|---|---|---|---|---|---|---|
| | −2 | −4 | −15 | −18 | −19 | −20 | −28 | −29 | −30 | −31 | −32 | −42 | −43 | −44 | −45 | −47 | −49 |
| **1**/$Fe^+$ | 2 | | 59 | 35 | | | | | 3 | 1 | | | | | | | |
| **1a**/$Fe^+$ | 4 | 1 | 9 | 77 | | 4 | | | 3 | 1 | 1 | | | | | | |
| **2**/$Fe^+$ | | | | 94 | | | 2 | 3 | | | | | | 1 | | | |
| **2a**/$Fe^+$ | | | | 67 | 26 | | 1 | 1 | 1 | 2 | | | | 1 | 1 | | |
| **2b**/$Fe^+$ | | | | 64 | 26 | | 1 | 2 | 2 | | 3 | | | 1 | | 1 | |
| **3**/$Fe^+$ | | | | 93 | | | | | | | | 2 | 5 | | | | |
| **3a**/$Fe^+$ | | | | 61 | 33 | | | | | | | 1 | 2 | 3 | | | |
| **3b**/$Fe^+$ | | | | 3 | 90 | 1 | | | | | | | 1 | 5 | | | |
| **3c**/$Fe^+$ | | | | 58 | 36 | | | | | | | 1 | 2 | | | 1 | 2 |
| **4**/$Fe^+$ | | | 100 | | | | | | | | | | | | | | |
| **4a**/$Fe^+$ | | | 61 | 39 | | | | | | | | | | | | | |

[a] Intensities are normalized to Σreactions = 100%. For the sake of clarity, intensities less than 1% are omitted.

bond of the methanol moiety in **12** leads to methyl loss. (iii) Activation of one of the C–H bonds in the formaldehyde ligand of **12** together with a multistep migration of the methanolic $CH_3$ group in **12** results in the formation of water together with acetaldehyde/$Fe^+$ as the ionic product.

Since the bond dissociation energies of the O–O bonds of organic peroxides do not vary substantially for alkyl substituents other than methyl, we assume that initial O–O insertion[21,22] of the $Fe^+$ cation occurs also for all peroxides studied here, leading to bis(alkoxide)/$Fe^+$ complexes $(RO)Fe(OR')^+$ as common intermediates.

The organization of the next sections is such that we will first focus on the reactions by which the major neutral products are formed, i.e. water, methyl, and methane, and will discuss the principal mechanistic features. Later on we will apply thermodynamic and kinetic criteria in order to uncover structure/reactivity patterns aimed at providing a more general understanding of which intermediates are crucial in the unimolecular dissociations of dialkyl peroxide/$Fe^+$ complexes.

**The Mechanism of Water Formation.** Water loss ($\Delta m$ = 18) dominates the MI spectra of the diethyl peroxide/$Fe^+$ and diisopropyl peroxide/$Fe^+$ complexes (Table 1). Based on the investigation of the isotopologues of **2** and **3** (Chart 1), the following mechanism is suggested: A metal-mediated transfer of an α-hydrogen atom from one alkoxy ligand to the oxygen atom of the other gives rise to bis-ligated intermediates **13** and **14**. The intermediacy of, for example, **13** was further probed by generating **13** independently by chemical ionization of a mixture of $Fe(CO)_5$, ethanol, and acetaldehyde. The MI mass spectrum (Table 2) of the so-formed ions is practically identical with that of **2**/$Fe^+$. This finding lends support to the conclusion that **13** serves as an intermediate in the course of the water elimination from **2**/$Fe^+$. Similar to the formation of $(CH_2O)Fe(CH_3OH)^+$ (**12**) from **1**/$Fe^+$, the rearrangements **2**/$Fe^+$ → **13** (and also **3**/$Fe^+$ → **14**) can be regarded as intramolecular disproportionations of the peroxides. However, in contrast to **12**, the intermediates **13** and **14** bear β-hydrogen atoms within the alcohol moiety. Thus, 1,2-eliminations of water from the alcohol ligands are feasible to give rise to the tris-ligated complexes **18** and **19**. These processes follow an accepted mechanism,[23] which proceeds *via* insertion of the metal ion into the alcoholic C–O bond and subsequent β-hydrogen shift from the metal-bound alkyl group to the metal center. Obviously, in **18** and **19**, the water ligand represents the most weakly bound

**Scheme 2**

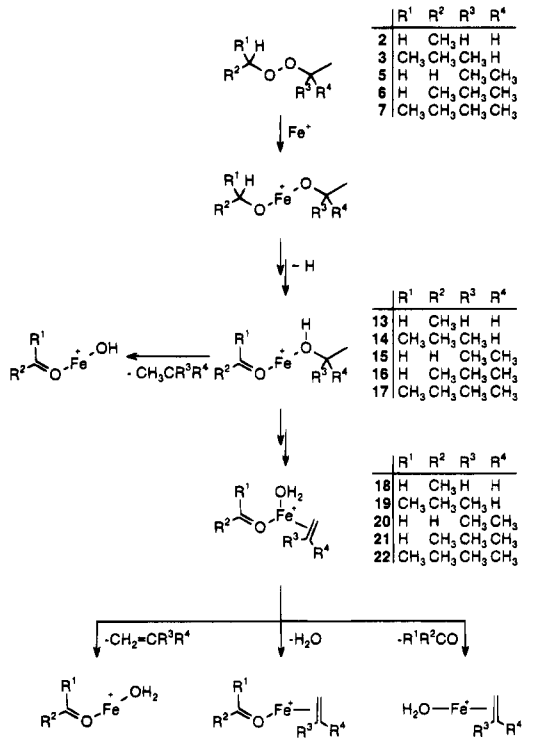


**Table 2.** Mass Differences ($\Delta m$ in amu) Observed in the MI Mass Spectra of **13**/$Fe^+$ − **13b**/$Fe^+$ Generated from $Fe(CO)_5$, Acetaldehyde, and Ethanol-$d_0$, *-1,1-*$d_2$, or *-2,2,2-*$d_3$, respectively[a]

| | $\Delta m$ | | | | | | | |
|---|---|---|---|---|---|---|---|---|
| | −18 | −19 | −28 | −29 | −30 | −31 | −32 | −44 |
| **13**/$Fe^+$ | 93 | | 1 | 4 | | | | 2 |
| **13a**/$Fe^+$ | 77 | 16 | | | 1 | 5 | | 1 |
| **13b**/$Fe^+$ | 41 | 50 | | | 1 | | 7 | 1 |

[a] Intensities are normalized to Σreactions = 100%; intensities less than 1% are omitted.

ligand;[24] consequently, water loss dominates in the MI spectra of **2**/$Fe^+$ and **3**/$Fe^+$.

From the $Fe^+$ complexes of the asymmetrically deuterated isotopologues **2a,b** and **3a,c**, $H_2O$ ($\Delta m$ = 18) and HDO ($\Delta m$ = 19) are formed, which is in line with this mechanistic picture. For example, if in **2a**/$Fe^+$, a hydrogen atom is transferred from the unlabeled ethyl group to the oxygen atom of the labeled ethoxy ligand, loss of $H_2O$ is expected, while, *vice versa*, transfer of a deuterium atom should lead to HDO formation. Interestingly, **2a**/$Fe^+$ and **2b**/$Fe^+$ both lead to losses of $H_2O$

(22) Similarly, an insertion of $Co^+$ into the weak N–O bond of methyl nitrite has been reported: Cassady, C. J.; Freiser, B. S.; McElvany, S. W.; Allison, J. *J. Am. Chem. Soc.* **1984**, *106*, 6125.

(23) (a) Allison, J.; Ridge, D. P. *J. Am. Chem. Soc.* **1976**, *98*, 7445. (b) Huang, S.; Holman, R. W.; Gross, M. L. *Organometallics* **1986**, *5*, 1856. (c) Prüsse, T. Ph.D. Thesis, Technische Universität Berlin D83, 1992.

(24) Schröder, D.; Schwarz, H. *J. Organomet. Chem.*, in press.

**Scheme 3**

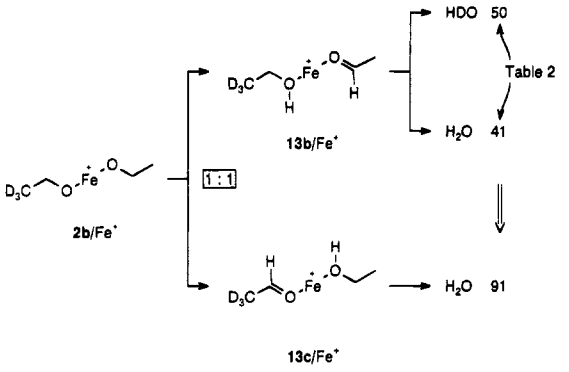


| | Predicted for 2b/Fe+ based on the MI data for 13b/Fe+ | Observed for 2b/Fe+ |
|---|---|---|
| $\frac{H_2O}{HDO}$ ratio | $\frac{91+41}{50} = 2.6$ | $\frac{64}{26} = 2.5$ |

and HDO in a constant ratio of ca. 2.5:1. Similarly, $H_2O$ and HDO are formed from labeled **3a**/$Fe^+$ and **3c**/$Fe^+$ in a ratio of ca. 1.8:1. Although one might be tempted to suggest competing 1,1- and 1,2-eliminations as an explanation for these similarities, earlier studies[23c,25] point to the operation of H/D-exchange processes. For example, it was demonstrated that the $Fe^+$-mediated dehydration of ethanol and other alcohols is associated with partial H/D exchange involving the hydrogen atoms of the alkyl backbone, while the OH proton hardly takes part. To test if this holds true for the proposed intermediate **13** as well, the isotopologues **13a** and **13b** were generated from $Fe(CO)_5$, acetaldehyde, and ethanol-*1,1-d*$_2$ or -*2,2,2-d*$_3$, respectively. In good agreement with the proposed H/D-exchange reactions, both exhibit $H_2O$ and HDO losses (Table 2); elimination of $D_2O$ is not observed, thus excluding the participation of the OH proton in the H/D exchange. It should be noted, however, that the MI spectra of **13a** and **13b** are not identical with those of **2a**/$Fe^+$ and **2b**/$Fe^+$; this finding is an immediate consequence of the fact that, on symmetry grounds, **13a** and **13b** each represent only one of the two conceivable intermediates formed en route from either **2a**/$Fe^+$ or **2b**/$Fe^+$. As exemplified in Scheme 3 for **2b**/$Fe^+$, this precursor gives rise in a 1:1 ratio to the intermediates **13b** and **13c**. From a simple calculation using the MI data (Table 2) for independently generated **13b**, it follows that the ratio of (combined) $H_2O$:HDO losses amounts to 2.6; this is in good agreement with the experimental figure of 64:26 = 2.5 derived from the data given in Table 1 for the $H_2O$:HDO losses from **2b**/$Fe^+$. From a similar analysis for the isotopologue **2a**/$Fe^+$, a primary kinetic isotope effect of ca. 6 can be derived for the transfer of an α-hydrogen atom from one ethoxy ligand to the other. This value is in excellent agreement with that reported for the analogous hydrogen shift in **1**/$Fe^+$.[12] For **14**, the central intermediate in the decompositions of **3**/$Fe^+$, a similar situation is assumed to prevail. In line with the finding that the OH proton is hardly involved in H/D exchanges, the MI spectrum of **3b**/$Fe^+$ shows a rather selective formation of HDO with only minor contributions of H/D-exchange products (Table 1).

**Methyl Loss and β-Methyl Shift.** Di-*tert*-butyl peroxide **4** does not bear α-hydrogen atoms. Therefore, the β-hydrogen shifts following O−O bond insertion as observed for **1**/$Fe^+$, **2**/$Fe^+$, and **3**/$Fe^+$ cannot take place. Instead, the cleavage of one of the C−C bonds gives rise to methyl loss ($\Delta m$ = 15) resulting in the formation of **24** as the ionic product. The mechanism of this process is depicted in Scheme 4 for the isotopologue **4a**/$Fe^+$; a secondary KIE of 1.56 for the losses of $CH_3^\bullet$ and $CD_3^\bullet$ is observed which corresponds to a value of 1.06 per deuterium atom in the *tert*-butyl groups.

Upon collisional activation, in addition to the expulsion of a methyl radical, **4**/$Fe^+$ gives rise to the formation of $[Fe,C_4,H_9,O]^+$ ions (Table 3), which formally correspond to the elimination of a *tert*-butoxy radical ($\Delta m$ = 73). Interestingly and unexpectedly, the CA spectrum of **4a**/$Fe^+$ (Figure 1a,b) does not only exhibit signals due to losses of *tert*-butoxy-$d_0$ and -$d_9$ groups (i.e., $\Delta m$ = 73 and 82), as would have been expected for the direct collision-induced dissociation of the inserted species **23a**; rather, signals arising from formal losses of $d_3$- and $d_6$-labeled *tert*-butoxy radicals are observed ($\Delta m$ = 76 and 79). At first sight, this finding seems to indicate a partial scrambling of methyl groups, which would demand a high-valent intermediate bearing two methyl groups at the metal center, i.e. $((CH_3)_2$-

**Scheme 4**

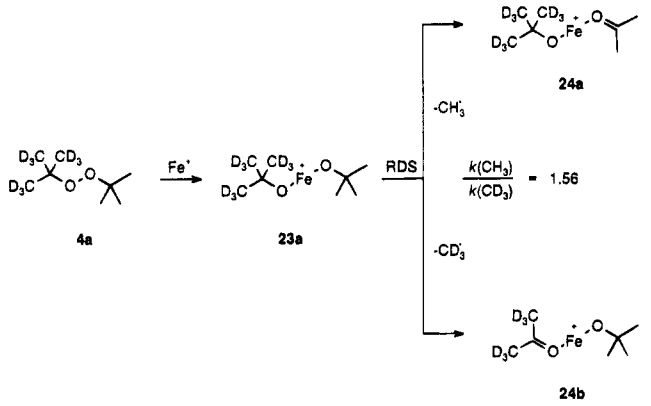


**Table 3.** Mass Differences ($\Delta m$ in amu) Observed in the CA Mass Spectra of **4**/$Fe^+$ and **4a**/$Fe^+$[a]

| | Δm | | | | | | | | |
|---|---|---|---|---|---|---|---|---|---|
| | −15 | −18 | −73 | −76 | −79 | −82 | $FeCD_3^+$ | $FeCH_3^+$ | $Fe^+$ |
| **4**/$Fe^+$ | 100 | 9 | | | | | 1 | 1 | |
| **4a**/$Fe^+$ | 100 | 66 | 6 | 4 | 5 | 4 | 1 | 1 | 1 |

[a] Intensities are given relative to the base peak = 100%; intensities less than 1% are omitted.

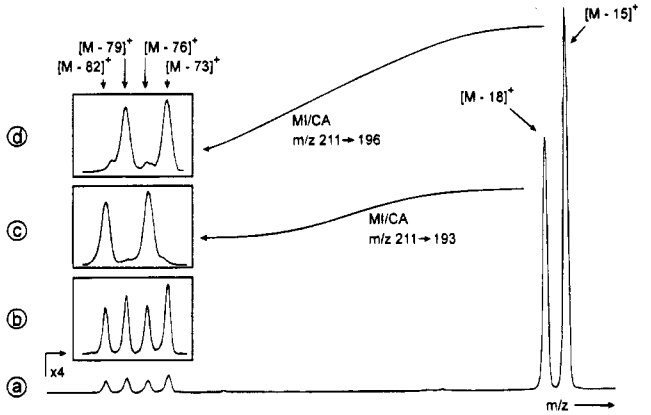


**Figure 1.** (a) Partial CA mass spectrum of **4a**/$Fe^+$ (mass range: *m/z* 120−200; B2 scan). (b) Detail of the CA mass spectrum of **4a**/$Fe^+$ magnified four times. (c) Detail of the MI/CA mass spectrum of **24a** generated by unimolecular $CH_3^\bullet$ loss from **4a**/$Fe^+$ (E2 scan). (d) Detail of the MI/CA mass spectrum of **24b** generated by unimolecular $CD_3^\bullet$ loss from **4a**/$Fe^+$ (E2 scan). The peak width in (a) differs from those in c and d due to the different scan methods.

(25) (a) Allison, J.; Ridge, D. P. *J. Am. Chem. Soc.* **1979**, *101*, 4998. (b) Prüsse, T.; Schwarz, H. *Organometallics* **1989**, *8*, 2856. (c) Schröder, D.; Zummack, W.; Schwarz, H. *J. Am. Chem. Soc.* **1994**, *116*, 5857.

**Table 4.** Mass Differences ($\Delta m$ in amu) Observed in the MI/CA Spectra of [**4**/$Fe^+$ − $CH_3$], [**4a**/$Fe^+$ − $CH_3$], and [**4a**/$Fe^+$ − $CD_3$][a]

| | $\Delta m$ | | | | | | | | | | | | |
|---|---|---|---|---|---|---|---|---|---|---|---|---|---|
| | −16 | −17 | −19 | −20 | −58 | −61 | −64 | −73 | −76 | −79 | $FeCD_3^+$ | $FeCH_3^+$ | $Fe^+$ |
| [**4**/$Fe^+$ − $CH_3$] | 12 | | | | 100 | | | 21 | | | | 8 | 3 |
| [**4a**/$Fe^+$ − $CH_3$] | | | 15 | 13 | 100 | 9 | 95 | 19 | 3 | 28 | 10 | 1 | 4 |
| [**4a**/$Fe^+$ − $CD_3$] | 16 | 14 | | | 100 | 7 | 92 | 25 | 3 | 18 | 1 | 11 | 5 |

[a] Intensities are given relative to the base peak = 100%. For the sake of clarity, some minor processes are omitted.

**Scheme 5**

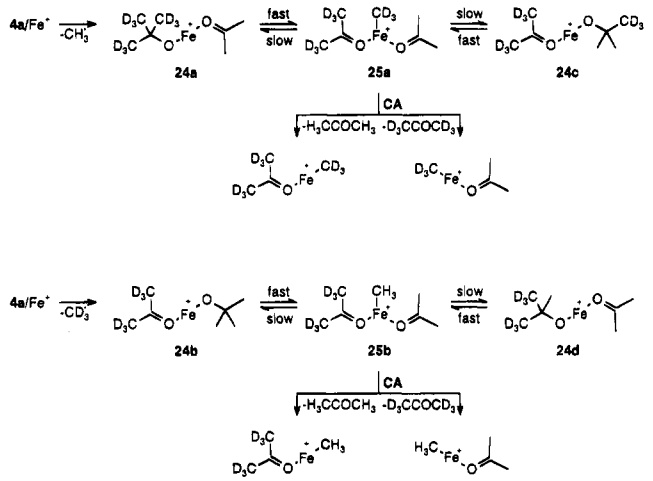


**Scheme 6**

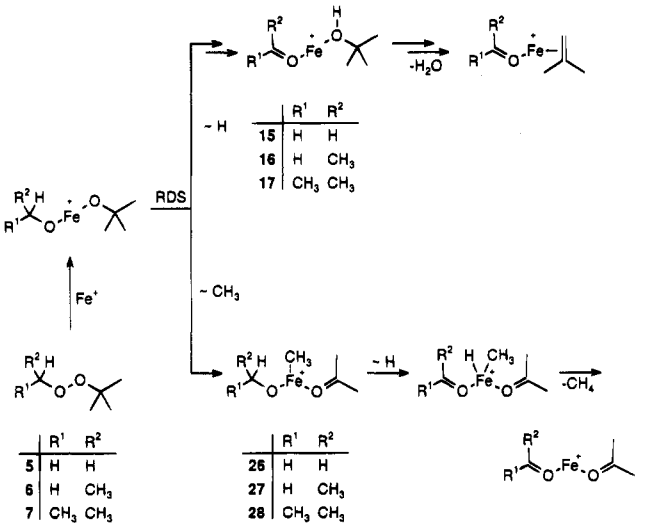


$CO)_2Fe(CH_3)_2^+$ and its corresponding isotopologues. Based on previous work of Schultz and Armentrout[26a] and more recent theoretical studies by Koch and co-workers[26b] on $Fe(CH_3)_2^+$, these intermediates are expected to decompose by reductive elimination of ethane rather than by losses of "scrambled" *tert*-butoxy radicals. Therefore, we contemplated whether in the CA experiment the $[Fe,C_4,H_9,O]^+$ ions are formed from **4**/$Fe^+$ by a combination of consecutive losses of a methyl radical and of acetone.

As an experimental test for this proposal, MI/CA experiments (Table 4) were performed such that the primary fragment ions corresponding to the methyl loss ($\Delta m$ = 15) from **4**/$Fe^+$ were collisionally activated. Indeed, in the MI/CA spectrum of [**4**/$Fe^+$ − 15], the loss of acetone ($\Delta m$ = 58) represents the base peak. The same experiment conducted with the ions [**4a**/$Fe^+$ − 15] and [**4a**/$Fe^+$ − 18], respectively, reveals in both cases losses of acetone-$d_0$ and -$d_6$ with quite similar intensities (see also Figure 1c,d), while acetone-$d_3$ is formed only to a minor extent. The superposition of these two MI/CA spectra clearly accounts for the four peaks observed in the CA spectrum of **4a**/$Fe^+$ (Figure 1a,b) and easily explains the observed alternating intensities for the formal butoxy radical losses (Table 3), which reflect the KIEs associated with methyl radical and acetone losses. Thus, the following mechanistic picture emerges (Scheme 5): After $CH_3^\bullet$ loss from **4a**/$Fe^+$, ion **24a** bearing a *tert*-butoxy-$d_9$ ligand undergoes a rapid $\beta$-$CD_3$ shift to the metal center to produce **25a**, which decomposes by losses of either acetone-$d_0$ or -$d_6$. Analogously, $CD_3^\bullet$ loss from **4a**/$Fe^+$ leads to **24b**, which rearranges by transfer of a $CH_3$ group to the metal ion. The so-formed intermediate **25b** decomposes *via* losses of acetone-$d_0$ or -$d_6$ as well. A related reversible $\beta$-methyl shift in **24b** has been observed previously in the ion/molecule reaction of $FeOC(CH_3)_3^+$ with labeled acetone; in this study[27] it was further demonstrated that a complete equilibration of the methyl groups is hindered by a slow transfer of the metal-bound methyl group to one of the acetone ligands. In the same manner, methyl scrambling in **24a−d** can hardly compete with acetone losses but accounts for the small amount of acetone-$d_3$ which is formed in the MI/CA experiments. It should be noted that upon collisional activation of **24a** a $FeCD_3^+$ fragment is formed with an intensity of 10%, corresponding to the loss of both acetone ligands from **25a**, while the $FeCH_3^+$ fragment is 10 times less intense (Table 4). *Vice versa*, **24b** gives rise to much more $FeCH_3^+$ (11%) as compared to $FeCD_3^+$ (1%). These findings further support structures **25a,b** as intermediates and exclude a rapid interchange of the methyl groups, which would result in more or less statistical amounts of both $FeCH_3^+$ and $FeCD_3^+$.

**Competing Pathways for the Generation of Methane and Water.** While the metastable decomposition reactions of the symmetric complexes **2**/$Fe^+$ and **3**/$Fe^+$ are dominated by losses of water, in the *tert*-butyl-substituted homologues **5**/$Fe^+$, **6**/$Fe^+$, and **7**/$Fe^+$, methane and water losses compete with each other. In this series, the ratios of methane and water losses drastically change from 8.5:1 for **5**/$Fe^+$ to 1:11 for **6**/$Fe^+$ and 1:19 for **7**/$Fe^+$.

The formation of water follows the mechanism discussed above (Scheme 2) with the distinction that, as compared to **2**/$Fe^+$ and **3**/$Fe^+$, due to the *tert*-butyl substituent, a hydrogen shift from the α-position is possible in one direction only. From the intermediates **15−17** in Schemes 2 and 6, water is eventually eliminated, containing a hydrogen atom from the *tert*-butoxy group. From **6c**/$Fe^+$ and **7b**/$Fe^+$, only $H_2O$ is formed, thus ruling out 1,2-eliminations from the ethyl or isopropyl groups, as this would also lead to HDO. As also observed for the isotopologues of **2**/$Fe^+$ and **3**/$Fe^+$, the generation of $H_2O$ from **5a**/$Fe^+$, **6a**/$Fe^+$, and **7a**/$Fe^+$ points to a partial H/D exchange with the hydrogen atoms of the *tert*-butyl substituents, in which the OH proton is involved to some extend as well. The intermediacy of the tris-ligated complexes **21** and **22** is suggested by the minor, but indicative, expulsion of isobutene ($\Delta m$ = 56) from **6**/$Fe^+$ and **7**/$Fe^+$, respectively.

(26) (a) Schultz, R. H.; Armentrout, P. B. *J. Phys. Chem.* **1992**, *96*, 1662. Also see: (b) Holthausen, M. C.; Fiedler, A.; Schwarz, H.; Koch, W. *Angew. Chem., Int. Ed. Engl.* **1995**, *34*, 2982.

(27) Schröder, D.; Schwarz, H. *Angew. Chem. Int. Ed. Engl.* **1990**, *29*, 910.

**Table 5.** Mass Differences ($\Delta m$ in amu) Observed in the MI Mass Spectra of $Fe^+$ Complexes of Asymmetric Dialkyl Peroxides **5**–**9** and their Isotopologues[a]

| | $\Delta m$ | | | | | | | | | | | | | | |
|---|---|---|---|---|---|---|---|---|---|---|---|---|---|---|---|
| | −2 | −3 | −15 | −16 | −17 | −18 | −19 | −28 | −29 | −30 | −32 | −44 | −45 | −47 | −56 |
| **5**/$Fe^+$ | | | 3 | 85 | | 10 | | | | 2 | | | | | |
| **5a**/$Fe^+$ | | | 4 | | 86 | 7 | 2 | | | | 1 | | | | |
| **6**/$Fe^+$ | | | | 8 | | 89 | | | | | | 1 | | | 2 |
| **6a**/$Fe^+$ | | | | | 23 | 13 | 60 | | | | | | 1 | | 3 |
| **6b**/$Fe^+$ | | | | 5 | 4 | 74 | 10 | | | | | 2 | 1 | | 4 |
| **6c**/$Fe^+$ | | | | 11 | | 86 | | | | | | | | 1 | 2 |
| **7**/$Fe^+$ | | | | 5 | | 93 | | | | | | | | | 2 |
| **7a**/$Fe^+$ | | | | | 3 | 25 | 70 | | | | | | | | 2 |
| **7b**/$Fe^+$ | | | | 3 | | 94 | | | | | | | | | 3 |
| **8**/$Fe^+$ | 1 | | 92 | | | 3 | | 2 | | 2 | | | | | |
| **8a**/$Fe^+$ | | 1 | | | | 97 | | 1 | | | 1 | | | | |
| **9**/$Fe^+$ | | | 94 | | | | | 3 | | 3 | | | | | |
| **9a**/$Fe^+$ | | | | | | 97 | 2 | | | 1 | | | | | |
| **10**/$Fe^+$ | | | | 3 | | 84 | | 3 | 10 | | | | | | |
| **10a**/$Fe^+$ | | | | 1 | | 14 | 71 | 2 | 12 | | | | | | |

[a]Intensities are normalized to Σreactions = 100%. For the sake of clarity, intensities less than 1% are omitted.

Concerning the mechanism of methane loss, we assume that after initial O–O bond insertion of the metal a $\beta$-methyl shift from the *tert*-butoxy ligand to the iron center takes place to generate the intermediates **26**–**28** (Scheme 6). Obviously, the metal-bound $CH_3$ group is not transferred to the oxygen atom of the second alkoxy ligand, since losses of the corresponding methyl ethers are neither observed in the MI nor in the CA mass spectra. This observation also excludes a direct reductive elimination of methyl ethers from **26**–**28**. Instead, a $\beta$-H shift from the alkoxy moiety to the metal center is suggested to occur; subsequently methane is reductively eliminated, giving rise to $(R^1R^2CO)Fe(OC(CH_3)_2)^+$ complexes ($R^1$, $R^2$ = H, $CH_3$). The mechanistic picture depicted in Scheme 6 further implies that the competition between methane and water losses can be traced back to competing hydrogen and methyl shifts, which represent the rate-determining steps (RDSs) of the two pathways. If this proposal holds true, one expects losses of $CH_4$, $CH_3D$, $H_2O$, and HDO from **6b**/$Fe^+$, which allow the determination of the kinetic isotope effects for both the methane and the water loss without interfering with each other. An approximate 1:1 ratio is expected for the $CH_4$ and $CH_3D$ losses, since the $CH_3$ shift should not be affected by a KIE, whereas water formation should reveal a distinct isotope effect, as it involves a rate-determining hydrogen transfer. This is indeed observed experimentally (Table 5): the intensities for losses of $CH_4$ and $CH_3D$ exhibit only a small KIE (1.25), while the $H_2O$:HDO ratio amounts to 7.4:1; even if partial H/D exchange is taken into account, this value reveals that water loss is affected by a substantial (and primary) KIE. Further support for a direct competition between $CH_3$ and H transfers is provided by the observation of isotopically sensitive branching[28] for **6**/$Fe^+$: upon α-deuteration of the ethyl group, the overall methane:water ratio drops from 1:11 for unlabeled **6**/$Fe^+$ to 1:3.2 for **6a**/$Fe^+$. This finding can be rationalized by the operation of a KIE, in that D transfer from the ethoxy to the butoxy ligand is slowed, while methyl transfer is less affected. Thus, due to direct competition between both processes, the elimination of $CH_3D$ gains in importance, while the intensity of the water loss decreases.

**Direction of the Initial H Shift.** While a consideration of the direction of the H transfer succeeding O–O bond insertion is not relevant for the iron complexes of the symmetric peroxides **1**, **2**, and **3**, in the *tert*-butyl-substituted complexes **5**/$Fe^+$, **6**/$Fe^+$, and **7**/$Fe^+$, the hydrogen shift is only possible from the α-position of R and, as demonstrated in the preceeding section, competes with a methyl shift from R′. In contrast, **8**/$Fe^+$, **9**/$Fe^+$, and **10**/$Fe^+$ are substituted asymmetrically and bear α-hydrogen atoms on either alkyl substituent. Thus, hydrogen transfers from the α-positions can proceed in two directions and, depending on its origin, would lead to different products. In fact, the product and labeling distributions obtained for **8a**/$Fe^+$, **9a**/$Fe^+$, and **10a**/$Fe^+$ should reveal directional preferences of the hydrogen migration in the metal-mediated decomposition of dialkyl peroxides.

Surprisingly, in the MI mass spectra of **8**/$Fe^+$ and **9**/$Fe^+$, losses of methyl radicals ($\Delta m$ = 15) dominate with 92% intensity (Table 5). Upon deuteration (**8a**/$Fe^+$ and **9a**/$Fe^+$, respectively) only $CD_3^\bullet$ is lost ($\Delta m$ = 18), while C–C bond activation within the ethyl or isopropyl groups is not observed. As already known from the study of **1**/$Fe^+$, the methyl loss originates from the activation of a methanolic C–O bond.[12] Therefore, we conclude that the hydrogen shift exclusively proceeds from the ethyl or isopropyl α-positions, respectively, to the methoxy oxygen atom leading to methanol as the alcohol moiety in both cases. In contrast, if a hydrogen atom of the methoxy group would have been transferred, water losses, following the mechanism depicted in Scheme 2, were expected to occur; this is not the case for **9**/$Fe^+$. Further, the minor loss of water from **8**/$Fe^+$ cannot be ascribed to a 1,2-elimination because no HDO ($\Delta m$ = 19) is formed from **8a**/$Fe^+$. More likely and analogous to **1**/$Fe^+$, water is generated from **8**/$Fe^+$ *via* multiple C–H bond activation of the original methoxy group. Since the thermodynamic driving force for C–H bond activation of formaldehyde is larger than that of acetaldehyde (see below), in **1**/$Fe^+$, water formation can compete efficiently with the methyl loss, while the expulsion of a methyl radical dominates for **8**/$Fe^+$.

Finally, **10**/$Fe^+$ exhibits $\beta$-hydrogen atoms on both alkyl substituents, such that irrespective of the direction of the initial hydrogen transfer step the water loss can occur according to the mechanism as depicted in Scheme 2. However, the preferential loss of HDO from **10a**/$Fe^+$, which is five times more abundant as compared to the loss of $H_2O$, demonstrates that the hydrogen transfer proceeds preferentially from the isopropoxy moiety to the ethoxy group. Considering the contributions of H/D-exchange processes as discussed above and possible kinetic isotope effects, the preference for a hydrogen transfer from the isopropyl group will even be larger than the ratio of the HDO and $H_2O$ eliminations. In conclusion, in **8**/$Fe^+$ and **9**/$Fe^+$, the hydrogen atom is transferred exclusively from the

(28) Raabe, N.; Karrass, S.; Schwarz, H. *Chem. Ber.* **1994**, *127*, 261 and references therein.

higher substituted alkoxy group to the less substituted one, and for **10**/Fe$^+$, a distinct preference is found in favor of the same direction.

**Energetic Considerations.** Although detailed mechanisms for the unimolecular reactions of dialkyl peroxide/Fe$^+$ complexes have been described in the previous sections, the underlying principles that determine the reactivity of the different peroxide/Fe$^+$ complexes remain to be uncovered. In the following, we will discuss the role of energetic effects which may serve to better understand the unimolecular Fe$^+$-mediated peroxide decomposition.

As demonstrated by the isotopic labeling studies, the branching ratio of the peroxide decompositions is determined by the $\beta$-hydrogen versus $\beta$-methyl transfers, and the relative activation barrier is higher for a methyl transfer.[27] As a consequence, the hydrogen shift should be favored for all complexes (except **4**/Fe$^+$). This is indeed reflected by the data, e.g. the absence of methane losses from Fe$^+$ complexes of symmetric diethyl- or diisopropyl peroxides, although methyl shifts would have been possible.

The Fe$^+$ complexes of the asymmetric peroxides **8**−**10** reveal a distinct preference for the direction of the initial H shift in that it occurs preferentially from the more substituted alkyl group to the O atom of the less substituted one. As the hydrogen transfers quite likely involve comparable energy requirements for the transition structures for either direction, the Hammond postulate may be applicable, and consequently, to a first approximation, thermodynamic criteria can be used to rationalize the observed selectivities.

As an example, let us discuss the system **9**/Fe$^+$. The metal-free disproportionation of **9** to acetone and methanol is thermochemically favored by ca. 9 kcal/mol as compared to the formation of formaldehyde and isopropyl alcohol.[29] This difference in the exothermicities of these two reaction channels becomes even larger for the metal-induced decomposition, since the Fe$^+$−L bond dissociation energies (BDE) of the rearrangement products also contribute:[30] while the ligand bond energies only slightly vary for the different alcohols, the BDE values increase from 33 kcal/mol for formaldehyde/Fe$^+$ to 37 kcal/mol for acetaldehyde/Fe$^+$ and 41 kcal/mol for acetone/Fe$^+$, reflecting the expected effect of increasing methyl substitution at the carbonyl group.[24,29] In summary, the formation of $(CH_3\text{-}OH)Fe(OC(CH_3)_2)^+$ from **9**/Fe$^+$ is about 17 kcal/mol more exothermic than that of the isomeric complex $(CH_2O)Fe(HOCH\text{-}(CH_3)_2)^+$. Similar considerations can be applied to **8**/Fe$^+$ and **10**/Fe$^+$. In following the Hammond postulate, these thermodynamic differences affect the energy demand of the associated transition states and, thus, account for the preferred C−H bond activation of the larger substituent. However, the effects of product stability are not applicable for **7**/Fe$^+$, since both the hydrogen shift from the isopropyl and the methyl shift from the *tert*-butyl substituent lead to acetone as carbonyl ligand. Here, hydrogen transfer is once more favored over that of a methyl group of the *tert*-butoxy ligand, which highlights the lower barrier associated with H migration to the metal.

(29) Estimations of the thermochemistry of disproportionation reactions of peroxides are based upon data taken from the following: Lias, S. G.; Bartmess, J. E.; Liebman, J. F.; Holmes, J. L.; Levin, R. D.; Mallard, W. G. Gas-Phase Ion and Neutral Thermochemistry. *J. Phys. Chem. Ref. Data, Suppl. 1* **1988**, *17*. Additional data for organometallic species were taken from the following: Armentrout, P. B.; Kickel, B. L in *Organometallic Ion Chemistry*; Freiser, B. S., Ed.; Kluwer: Dordrecht, the Netherlands, in press.

(30) Assuming that synergistic effects between both ligands are negligible, a simple additivity scheme can be applied: Benson, S. W. *Thermodynamical Kinetics: Methods for the Estimation of Thermochemical Data and Rate Parameters*, 2nd ed.; Wiley: New York, 1976.

**Scheme 7**

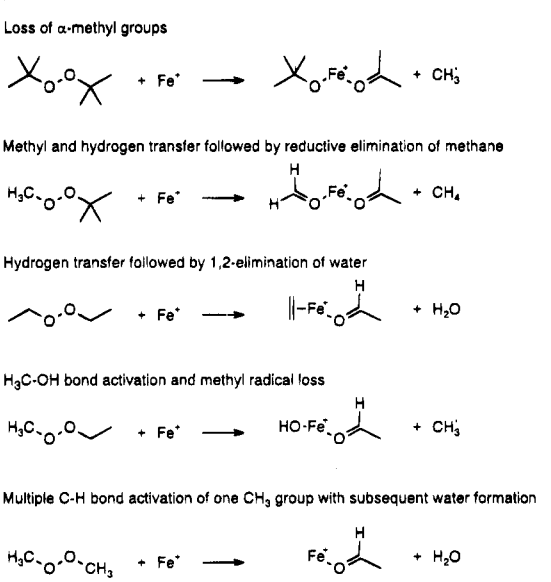


Consequently, water elimination represents the by far dominating reaction channel for **7**/Fe$^+$, while formation of methane is a minor process.

In conclusion, there are two important effects that influence the reactivity of dialkyl peroxide/Fe$^+$ complexes: (i) the relative barriers of hydrogen and methyl transfer steps and (ii) the stability of the rearranged products formed as intermediates in the course of the reaction. In the case of **2**/Fe$^+$, for example, both effects favor the same sequence: $\beta$-H shift is not only preferred due to a lower barrier but also gives rise to the more stable complex as compared with a $\beta$-methyl shift. Therefore, water is the by far major neutral product expelled from this complex, and methane loss is not observed in the unimolecular decay of metastable **2**/Fe$^+$. Even upon collisional activation of these ions the abundance of the methane loss is negligible. This indicates that indeed energetic reasons disfavor the methyl transfer in **2**/Fe$^+$. In contrast, for **5**/Fe$^+$, both effects compensate each other: while the barrier is lower for the $\beta$-H shift, transfer of a $\beta$-methyl group will lead to the more stable complex. Consequently, the losses of methane and water compete with each other. Accordingly, the changes of the methane:water ratios in the **5**/Fe$^+$−**7**/Fe$^+$ series are easily explained in terms of the increasingly favored exothermicities of the hydrogen shifts as compared to the methyl migrations.

**Structure/Reactivity Relationships.** In this study five mechanisms for the unimolecular decompositions of dialkyl peroxide/Fe$^+$ complexes have been derived from a combination of mass spectrometric methods with isotopic labeling (Scheme 7). These findings can be combined into a quite simple flow chart (Figure 2) which allows predictions about the major unimolecular decomposition channels of dialkyl peroxide/Fe$^+$ complexes simply based on the number of hydrogen atoms present in the α- and $\beta$-positions of the peroxides ROOR′ with R ≤ R′.

As depicted in Figure 2, four criteria are used to make predictions of the major reaction channel for a given peroxide/Fe$^+$ complex: (i) If R does not bear an α-hydrogen atom (i.e., R and R′ are *tert*-butyl groups), a methyl radical is lost (mechanism A). (ii) If R bears an α-H, but R′ does not, the competition between hydrogen and methyl shift leads to the expulsions of methane (mechanism B) and water (mechanism C). (iii) If both R and R′ bear α-hydrogen atoms and in addition R contains a $\beta$-H, water formation (mechanism C) from the alcohol fragment is the dominating process. (iv) If, instead, R

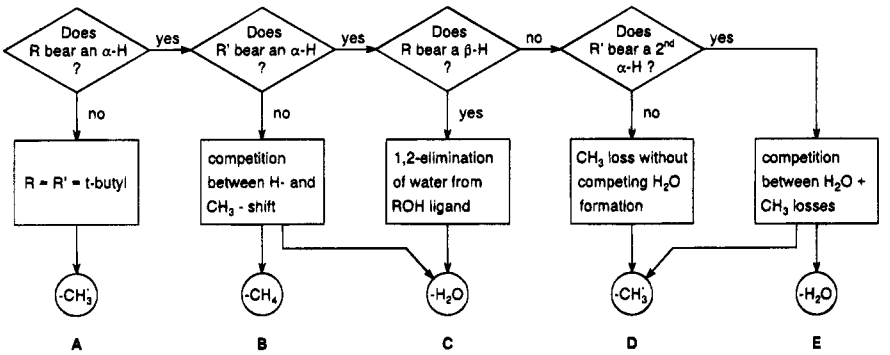


**Figure 2.** Flow chart for the qualitative prediction of the unimolecular reactivity of peroxide/$Fe^+$ complexes (R, R′ = Me, Et, *i*-Pr, *t*-Bu with R ≤ R′).

does not bear a $\beta$-H (R = $CH_3$), methyl loss (mechanism D) prevails but may compete with water loss (mechanism E), if a second α-hydrogen is located on R′. Although the flow chart is based upon qualitative energetic considerations as discussed above, it is quite advantageous that one does not need any detailed information about thermochemistry; rather, the scheme can be applied in a black-box manner in that a prediction of the major decomposition channel of dialkyl peroxide/$Fe^+$ complexes is possible from the knowledge of the peroxide structure only. *Vice versa*, one may apply this scheme for the analysis of the peroxides itself.

## Conclusions

The unimolecular decomposition reactions of dialkyl peroxides, complexed to bare $Fe^+$, can be traced back to five different mechanistic pathways which give rise to water, methane, and methyl radicals as neutral products. These processes are quite selective for each peroxide/$Fe^+$ complex, and side reactions do not play an important role. The initial insertion step of the metal ion into the weak O−O bond is common for all peroxides ROOR′. The ensuing fate of the insertion complexes is determined by the substitution patterns and can be rationalized by energetic arguments. In general, and not surprisingly, lower barriers and more exothermic intermediates and products are preferred, namely, transfer of hydrogen and formation of stable carbonyl compounds in the metal-mediated decomposition of peroxides.

The findings have been combined in a flow chart that allows a direct qualitative correlation between the structure of the peroxides and the reactivities as observed in the MI mass spectra of the corresponding $Fe^+$ complexes. This might be used as a predicting tool to probe the reactivity of other metal-induced reactions of peroxides.

**Acknowledgment.** Financial support by the Deutsche Forschungsgemeinschaft, the Volkswagen-Stiftung, and the Fonds der Chemischen Industrie is acknowledged.

JA951832D